

Figure S1

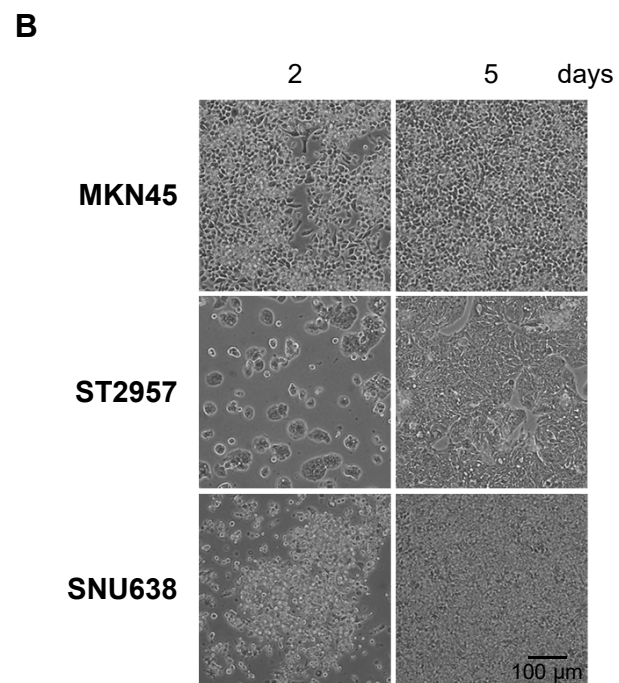
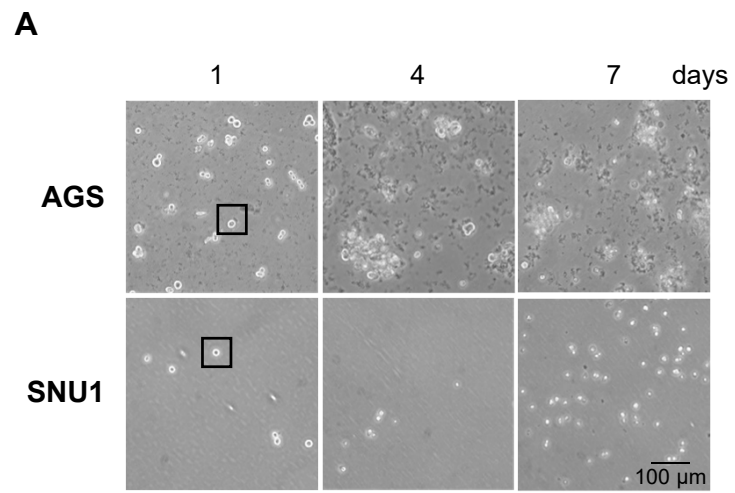
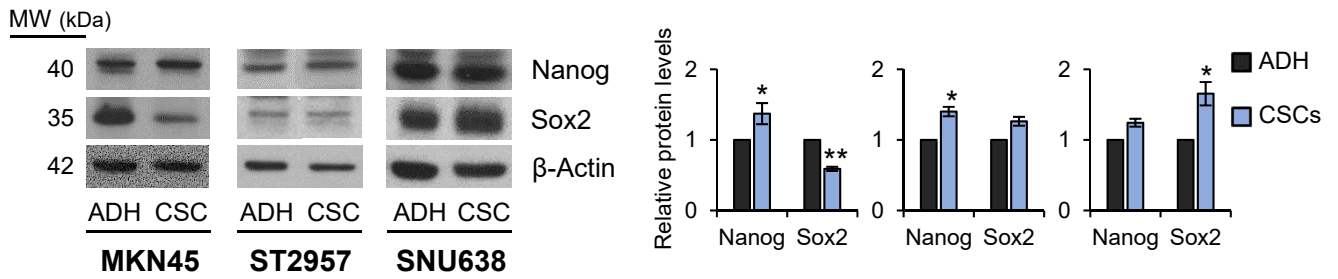
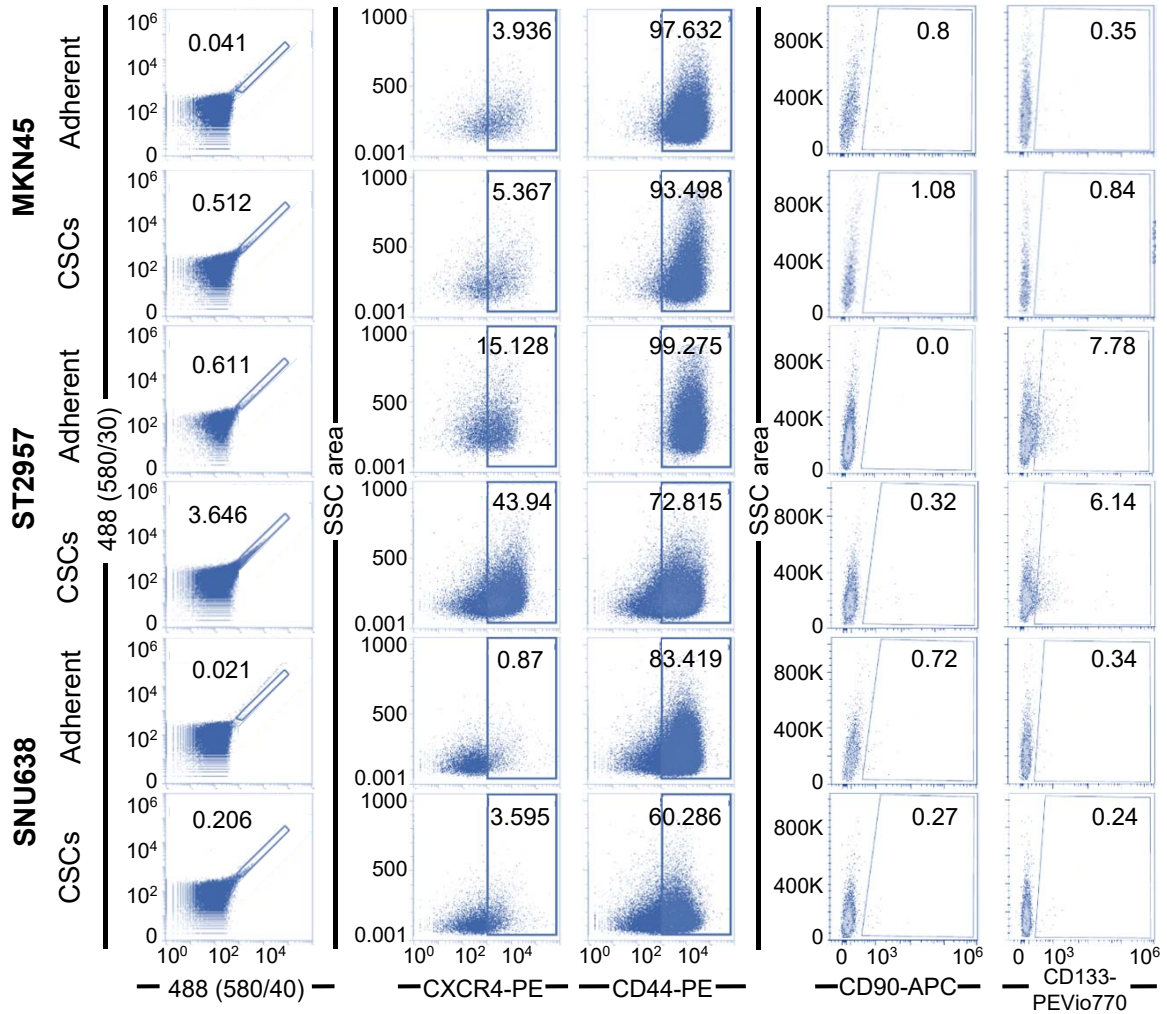


Figure S2

**A**



**B**



**C**

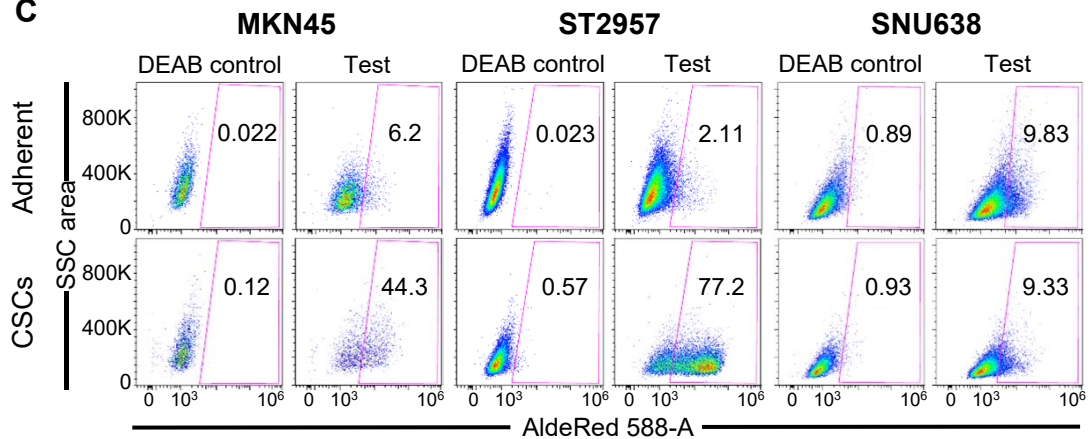


Figure S3

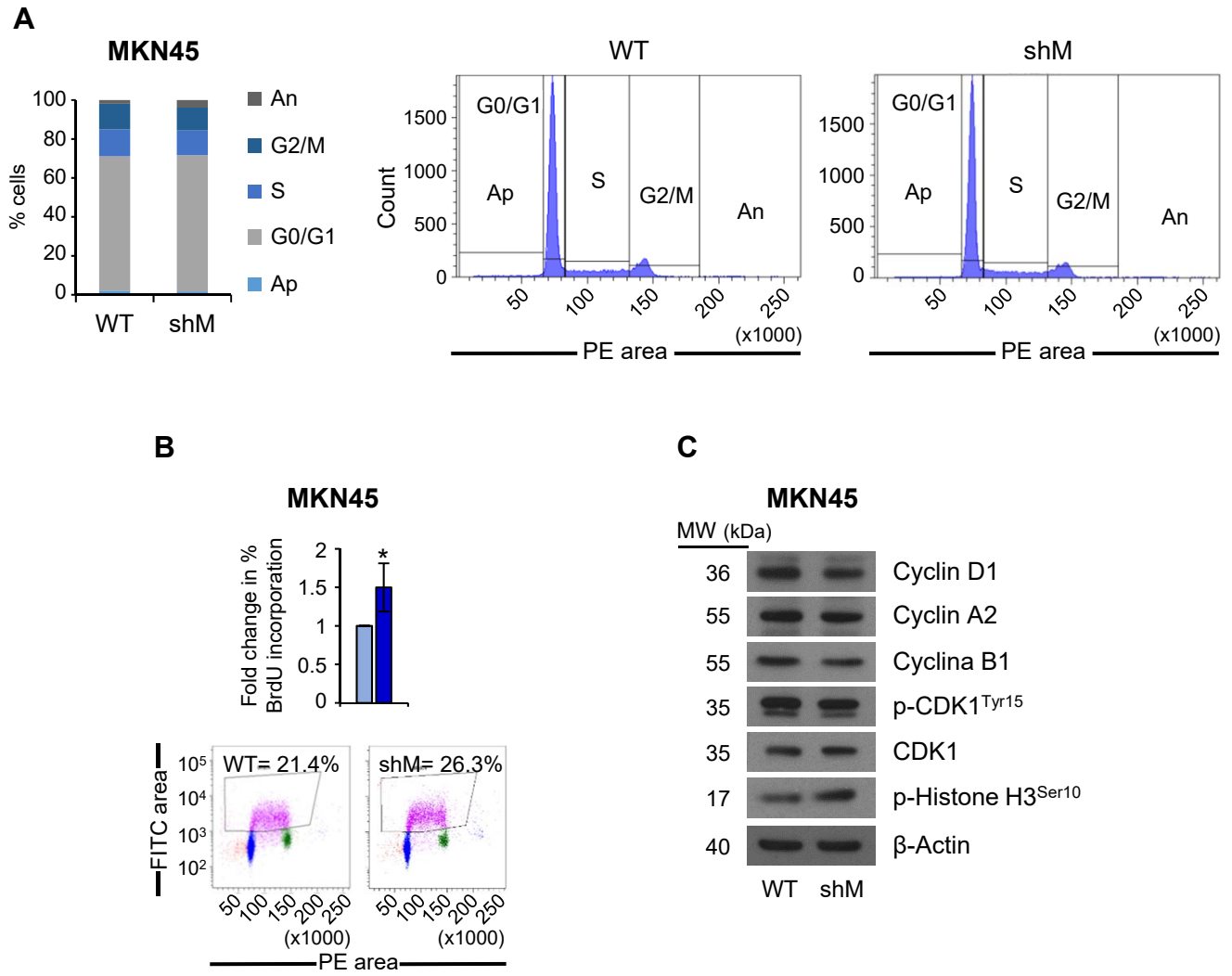
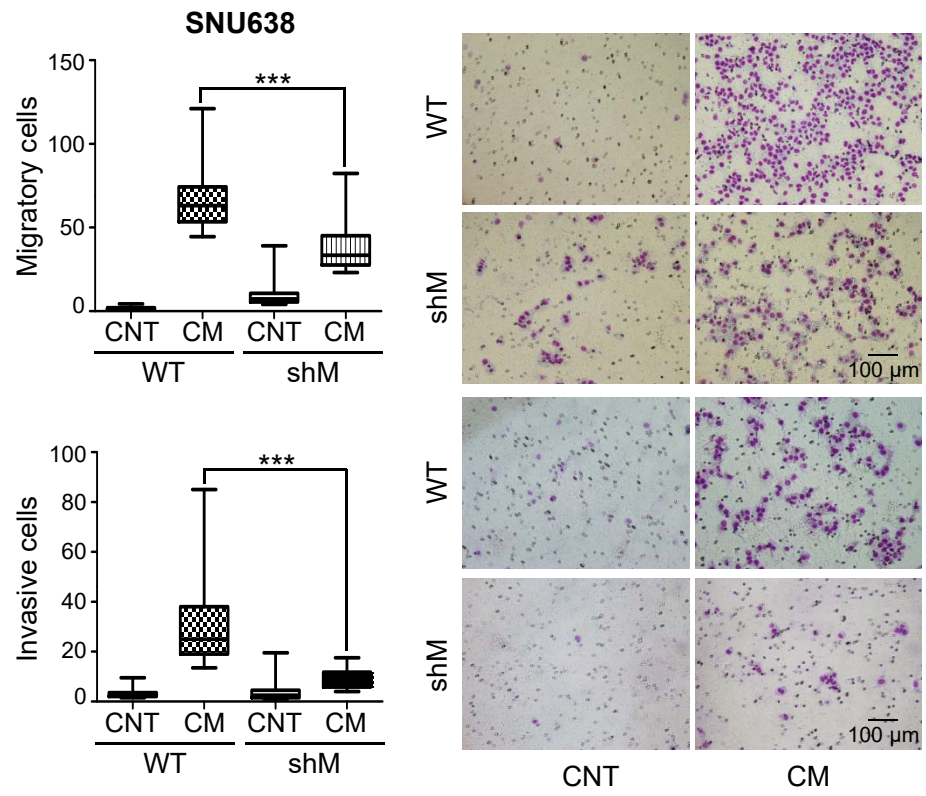


Figure S4



**Figure S1. Isolation of GCSCs from GC cell lines.** (A) Sphere formation assay of AGS and SNU1 GC cell lines. Cells were grown in ultra-low-attachment 6-well plates with DMEM/F-12 medium (3000 cells per well) containing specific supplements. Representative images were taken 1, 4 and 7 days later. Scale bar: 100  $\mu$ m. (B) Re-differentiation of CSCs from MKN45, ST2957 and SNU638 cell lines. CSCs were grown in adherent conditions with 10% FBS medium. Representative images were taken 2 and 5 days later. Scale bar: 100  $\mu$ m. The experiments were repeated two times with similar results.

**Figure S2. GCSCs characterization.** (A) Western blot analysis of NANOG and SOX2 in the GC cell lines MKN45, ST2957 and SNU638 cultured in adherence (ADH) or as sphere (CSCs). Right, graphs show the fold change of protein levels compared to ADH. Protein levels were normalized with  $\beta$ -actin. WB images are representative of the results obtained in three different experiments performed under the same conditions. The statistical significance was evaluated with two-tailed Student's t-test ( $*P < 0.05$ ;  $**P < 0.01$ ;  $***P < 0.001$ ). (B) Flow cytometric analysis of autofluorescence (580/30-580/40), CXCR4, CD44, CD90 and CD133 cell surface markers in the 3 GC cell lines and their CSCs. Representative plots with the percent-positive cells present within the single-cell, live and debris-free population are shown. (C) ALDH activity profile. The 3 GC cell lines and their CSCs were counter-stained with AldeRed to determine the frequency of ALDH-positive cells by flow cytometry. Representative plots are shown, in the presence or absence of the ALDH inhibitor (DEAB), with the percent-positive cells present within the single-cell, live and debris-free population.

**Figure S3. *MAD2L1* interference does not affect proliferation in MKN45<sup>CSCs</sup>.** (A) Cell cycle profile of MKN45<sup>CSCs</sup>. MKN45 2<sup>nd</sup> generation-enriched CSC cultures after *MAD2L1* interference (shM) or not (WT) were analyzed by flow cytometry. The graph

shows the percentage of cells in each phase of the cell cycle. An = aneuploidy (cells > 4n); G2/M = G2/mitosis; S = synthesis; G0/G1; Ap = apoptosis (cells < 2n). **(B)** BrdU incorporation analysis. MKN45<sup>CSCs</sup> WT and shM were incubated with BrdU (10  $\mu$ M) for 1 hour and analyzed by flow cytometry. Representative plots with the percent-positive cells present within the single-cell, live and debris-free population are shown. On top, histogram summarizing the percent of BrdU-positive cells in sphere cultures from three different experiments. Fold changes were calculated compared to WT. **(C)** Western Blot analysis for the cell cycle proteins Cyclin D1, Cyclin A2, Cyclin B1, p-CDK1<sup>Tyr15</sup>, CDK1 and p-Histone H3<sup>Ser10</sup> in MKN45<sup>CSCs</sup> WT and shM.  $\beta$ -actin was used as a loading control. The experiments were repeated three times with similar results. Statistical significance was evaluated with two-tailed Student's t-test (\* $P$  < 0.05).

**Figure S4. MAD2 levels regulate migration and invasion in SNU638<sup>CSCs</sup>.** Transwell migration (top) and invasion (bottom) assay in SNU638<sup>CSCs</sup> after MAD2 downregulation. Graphs show the quantification of stained migratory and invasive cells, respectively, from CSCs WT and shM using the transwell assay, without and with 20% serum-free conditioned medium from M2-differentiated human macrophages (CM) after 48 h. Representative photographs of the experiment on the right. Scale bar: 100  $\mu$ m. Three independent experiments were performed with similar results. The statistical significance was evaluated with one-way ANOVA, post hoc comparisons, Bonferroni's test (\*\*\* $P$  < 0.001).